Limit analysis of submerged slopes subjected to water drawdown

Chardphoom Viratjandr and Radoslaw L. Michalowski

Abstract: A rapid draw of water from a reservoir can cause a temporary increase in the hydraulic gradient that may not be tolerated by the slope of an earth dam. The increased seepage forces may lead to slope instability, causing the collapse of the structure. The kinematic approach of limit analysis is used to examine stability of slopes subjected to a rapid or slow drawdown. Combinations of slope inclination, soil properties, and hydraulic conditions are found for which the slope becomes unstable. The results are presented in the form of charts for convenient practical use, and the safety factors can be obtained from the charts without the need for iteration. For granular slopes, particularly if shallow, subjected to drawdown, a simple translational mechanism with a shallow failure surface is not the most adverse mechanism for all water-draw regimes.

Key words: slopes, stability, rapid drawdown, limit state analysis.

Résumé : La vidange rapide d'un réservoir peut causer une augmentation temporaire du gradient hydraulique qui ne puisse pas être toléré par la pente d'un barrage en terre. L'accroissement des forces d'infiltration peut conduire à l'instabilité de la pente causant une rupture de la structure. L'approche cinétique de l'analyse limite est utilisée pour examiner la stabilité des pentes assujetties à une vidange rapide ou lente. On a déterminé les combinaisons de l'inclinaison de la pente, des propriétés des sols et des conditions hydrauliques pour lesquelles la pente devient instable. Les résultats sont présentés sous la forme de graphiques pour une utilisation conventionnelle pratique; les coefficients de sécurité peuvent être obtenus à partir des graphiques sans besoin d'itération. On a trouvé que pour les pentes pulvérulentes, particulièrement les faibles pentes, soumises à une vidange, un simple mécanisme de translation avec une surface de rupture superficielle n'est pas le mécanisme le plus défavorable pour tout régime de rabaissement de nappes d'eau.

Mots clés : pentes, stabilité, vidange rapide, analyse d'état limite.

[Traduit par la Rédaction]

Introduction

Stability analysis of slopes subjected to rapid changes in hydraulic conditions is a necessary part of the design processes for drawing water from reservoirs and filling reservoirs with water. Morgenstern (1963) cites some of the earlier descriptions in the literature of failures of earth slopes caused by the drawdown of water from reservoirs. A rapid draw of water may cause large hydraulic gradients in the soil which, in turn, produce increased seepage forces that can destabilize a slope.

A set of charts for the stability of earth slopes during rapid drawdown was presented by Morgenstern (1963), who used a slice method to estimate the safety factor of slopes for a rapidly dropping water level. These changing hydraulic conditions were simplified to make the presentation of results possible for a wide range of parameters. A comprehensive discussion of methods for stability computations for a sudden drawdown was undertaken by Wright and Duncan (1987), who classified the methods into two groups: in the first group, pore-water pressure is evaluated first, and the strength of the soil is considered to be independent of the drawdown process; in the second group, the influence of consolidation stress on shear strength is considered. In a more recent publication, Wright and Duncan (2003) illustrate the computations of the second group. The charts of Morgenstern (1963) and the newer calculations by Lane and Griffiths (2000) fall within the first group, and the computational results in this paper also relate to constant strength during the drawdown process.

Both groups of analyses can be performed using a variety of calculation techniques, such as the limit equilibrium techniques, finite element method (FEM), or limit analysis. Earlier approaches included the limit equilibrium technique, whereas the FEM technique has been used more recently to analyze the same problem of stability under rapid drawdown (Lane and Griffiths 2000). The results in this paper have been obtained using the kinematic approach of limit analysis. The advantage of this latter method is that it gives a rigorous bound on the true solution to the problem, yet it is relatively easy to generalize the solution for a wide range of parameters describing the geometry of the slope and the soil

Received 25 August 2004. Accepted 17 March 2006. Published on the NRC Research Press Web site at http://cgj.nrc.ca on 19 July 2006.

C. Viratjandr[1] and R.L. Michalowski.[2] Department of Civil and Environmental Engineering, University of Michigan, 2340 G.G. Brown Building, 2350 Hayward, Ann Arbor, MI 48109-2125, USA.

[1]Present address: Department of Civil Engineering, Ubonratchathani University, Ubonratchathani Province, 34190, Thailand.

[2]Corresponding author (e-mail: rlmich@umich.edu).

 doi:10.1139/T06-042

strength. The hydraulic conditions need to be simplified, however, to make presentation of results consistent and manageable.

Ideally, the rate at which the water level in a reservoir drops down should be small enough that the phreatic surface within the slope closely follows this drop, producing a small gradient of the hydraulic head. This process is time-sensitive and depends on the hydraulic conductivity of the soil. An exact solution to the problem requires that a transient seepage problem be considered. Such calculations need to be specific for a given slope, with little chance for presentation of generalized charts. To make presentation of results manageable for a wide range of parameters, the safety factor is presented as a function of the relative position of the water level in the reservoir and the phreatic surface in the soil. Rather than solving for true distribution of the hydraulic head in the slope, however, a simplifying assumption is made that equipotentials remain vertical in a portion of the slope during rapid drawdown. Such an assumption corresponds to an instantaneous (fictitious) drawdown leading to an overestimation of the hydraulic gradients (conservative assumption).

During the operation of an earth dam, the difference in water level in the reservoir and in the soil of the slope needs to be judged based on the rate of water draw and on the hydraulic conductivity of the soil. This difference can also be monitored during drainage of the water from a reservoir, and the rate of draw can be adjusted to assure safe operation. The results presented in this paper focus on the stability of submerged slopes subjected to a rapid drop in the water level (drawdown but not filling). For an earth dam, this corresponds to the stability of the upstream slope during drawdown, and the authors do not claim to solve the comprehensive problem of earth dam stability.

This paper fills a gap in the design tools for partially submerged slopes subjected to water drawdown. The charts presented will allow the designer to directly obtain the safety factor for slopes subjected to a variety of drawdown regimes. The results of calculations are presented in the form of charts created in a manner that eliminates the need for iterations when the safety factor is sought. Safety factors for specific drawdown processes are compared with those calculated by Lane and Griffiths (2000), who used the finite element analysis to arrive at similar results.

A consideration of the pore-water pressure in the kinematical approach of limit analysis is reviewed in the next section, followed by stability analysis of a partially submerged earth slope. As an analysis for the purely granular soil becomes less elaborate, a closed-form solution is sought for this case in a separate section. Although a shallow translational mechanism is the most adverse collapse mode for dry granular slopes, this was not found to be true for submerged (particularly shallow) slopes. Lastly, stability charts are presented and the results are compared with those from the FEM. The paper concludes with brief remarks.

Pore-water pressure in limit analysis

Limit analysis is an approximate method for estimating limit loads that provides a strict lower or upper bound to the true limit load. Alternatively, problems can be formulated to obtain, for instance, an estimate of the critical height of a structure (such as a slope) or the material strength necessary to avoid collapse under a given set of loads. Here we apply this method to estimate a safe procedure for drawing down water in a reservoir bounded by an earth slope.

The method applied here is referred to as the kinematic approach of limit analysis. The soil is assumed to be perfectly plastic, with the yielding described by a convex function and the deformation governed by the normality rule. The method is based on the kinematic theorem that states: the rate of internal work D is not less than the rate of work of true external forces in any kinematically admissible mechanism.

$$[1] \qquad \int_V D(\dot{\varepsilon}_{ij}^{k}) \geq \int_S T_i v_i^{k}\, dS + \int_V X_i v_i^{k}\, dV$$

where T_i is a true traction vector on boundary S, X_i is the distributed load (e.g., the soil weight), V is the volume of the mechanism, and v_i^k is the velocity field vector in a kinematically admissible mechanism (with $\dot{\varepsilon}_{ij}^{k}$ being the strain rate tensor in a kinematically admissible velocity field). Throughout the rest of the paper we drop superscript "k" because all mechanisms considered are kinematically admissible. Hence, from a work (rate) balance equation one can calculate an upper bound to an active limit load, or a lower bound to a reaction. One could also calculate a lower bound to, for instance, the cohesion necessary to maintain stability of an earth structure. Here the method is used to find an upper bound to the difference in the water level in the reservoir and in a slope so that the hydraulic gradient does not cause the collapse of the structure. For that, one needs to introduce additional terms into inequality [1], which include the influence of the presence of water. These additional terms must account for the work of the buoyancy forces, seepage forces, and water pressure on the structure boundary.

To include explicitly the influence of water in the work balance equation, the yielding of the soil is described by a function of the effective stresses σ'_{ij}:

$$[2] \qquad f(\sigma'_{ij}) = 0$$

and the water pressure in the soil pores and in the reservoir is considered here as an external loading on the soil skeleton and on the boundary of the structure, respectively. Such an analysis was proposed earlier for slopes with a phreatic surface enclosed within the earth mass (Michalowski 1995). The analysis here, however, must be modified because of the submergence (or partial submergence) of the slope. To derive the terms in the work rate balance equation that account for the presence of water, consider derivative $\partial/\partial x_i$ of the product uv_i, where u is the pore-water pressure

$$[3] \qquad \frac{\partial}{\partial x_i}(uv_i) = \frac{\partial u}{\partial x_i} v_i + u \frac{\partial v_i}{\partial x_i}$$

where

$$[4] \qquad \frac{\partial v_i}{\partial x_i} = -\dot{\varepsilon}_{ii}$$

is the volumetric strain rate. The minus sign in eq. [4] appears because of the compression-positive sign convention. Now, writing eq. [3] for the volume of the entire mechanism, V, and after some transformation, one obtains

$$[5] \quad -\int_V u\dot{\varepsilon}_{ii}\,dV = \int_V \frac{\partial}{\partial x_i}(uv_i)\,dV - \int_V \frac{\partial u}{\partial x_i}v_i\,dV$$

$$= \int_S un_iv_i\,dS - \int_V \frac{\partial u}{\partial x_i}v_i\,dV$$

where S is the surface bounding volume V, and n_i is the outward unit vector perpendicular to surface S. The divergence theorem was used to transform the first integral on the right-hand side of eq. [5] into the surface integral. The water pressure u in eq. [5] can be represented as a function of the hydraulic head h. With the omission of the kinetic part, the hydraulic head is

$$[6] \quad h = u/\gamma_w + Z$$

where γ_w is the unit weight of water, and Z is the elevation head. Substituting the pore pressure u from eq. [6] into eq. [5] yields

$$[7] \quad -\int_V u\dot{\varepsilon}_{ii}\,dV = \int_S un_iv_i\,dS - \gamma_w\int_V \frac{\partial h}{\partial x_i}v_i\,dV + \gamma_w\int_V \frac{\partial Z}{\partial x_i}v_i\,dV$$

The second term on the right-hand side represents the work of the seepage force ($-\gamma_w\partial h/\partial x_i$) in the entire mechanism, and the last term is the work of the buoyancy force. To include the influence of the water on the stability of a slope, the work of both seepage and buoyancy forces must be included in the analysis. These terms can be included explicitly or, based on eq. [7], one can write the work of water pressure (equal to the work of the seepage forces and buoyancy forces) as a sum of pore pressure work on skeleton expansion (dilatancy) and the work of the water pressure on boundary S:

$$[8] \quad \dot{W}_u = -\int_V u\dot{\varepsilon}_{ii}\,dV - \int_S un_iv_i\,dS$$

The first integral is the work of the pore pressure on the volumetric strain of the skeleton, and the second integral is the work of the water pressure on boundary S of the structure. The first term on the right-hand side is positive in the field with dilating soil, and the minus sign here comes from the compression-positive sign convention (compressive pore pressure does positive work on the skeleton expansion). The result in eq. [8] is that obtained earlier in Michalowski (1995). A more comprehensive discussion on application of eq. [8] in limit analysis can be found in Michalowski (1999).

To apply the kinematic theorem to stability analysis of a partly submerged slope with a known distribution of the pore-water pressure, the two terms in eq. [8] must be included in eq. [1], i.e.,

$$[9] \quad \int_V D(\dot{\varepsilon}_{ij})\,dV \geq \int_S T_iv_i\,dS + \int_V X_iv_i\,dV - \int_V u\dot{\varepsilon}_{ii}\,dV - \int_S un_iv_i\,dS$$

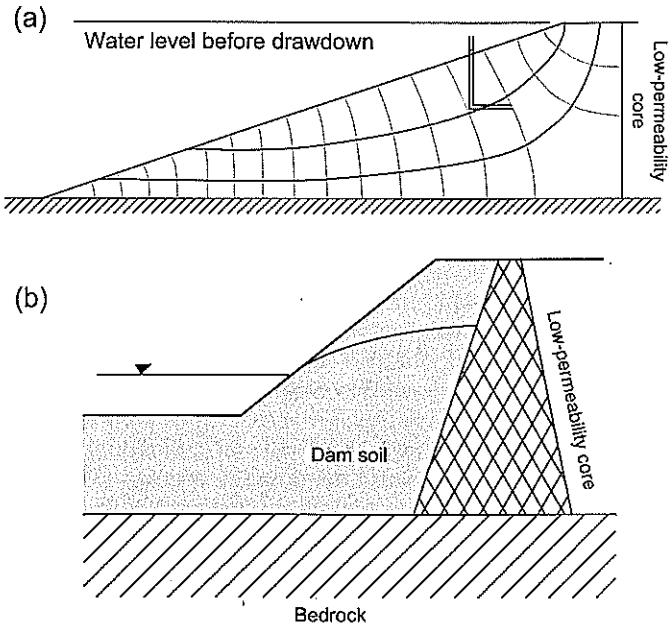

Fig. 1. Cross section of an earth dam: (*a*) flow net for drawdown state (after Terzaghi and Peck 1948); (*b*) schematic of an earth dam with a low-permeability core.

The forces X_i distributed over the volume are now specified as the material unit weight γ_i. A very rapid drawdown will then be modeled by an instant change in the water pressure on the slope surface and with a change in the pore-water pressure distribution within the slope. Very slow drawdown can be modeled as a simultaneous drop of the water in the reservoir and the phreatic surface in the slope.

Stability analysis of a submerged slope

An example of a submerged slope with a realistic distribution of equipotentials, immediately after the drawdown process, is shown in Fig. 1*a* (after Terzaghi and Peck 1948), and a fragment of an earth dam is presented schematically in Fig. 1*b*. The core of the dam in Fig. 1*b* is constructed of a low-permeability material (such as clay), whereas the slope is formed of a soil characterized by some cohesion (e.g., silty sand), or it may be built of a granular material. To account for the change in hydraulic conditions due to a rapid drawdown, one needs to first describe the pore pressure field immediately after drawdown. An accurate description of this pore pressure distribution requires solution of a transient seepage problem. Although this can be done effectively for a given set of conditions, generalization of such a solution cannot be done easily. To make the limit analysis calculations manageable and presentation of results possible for a wide range of parameters, a simplifying (but safe) assumption is introduced. Prior to drawdown, the potential is uniform throughout the saturated mass (Fig. 2*a*), and a fictitious (instantaneous) draining process is considered during which the equipotentials remain vertical within a portion of the slope (Fig. 2*b*), whereas the potential remains constant (but different) on both sides of that portion. Such an assumption, although not conforming to a solution of the Laplace equation describing the seepage problem, is conservative, as it

Fig. 2. Idealized hydraulic conditions: (*a*) before drawdown; (*b*) equipotentials during a fictitious (instantaneous) drawdown process.

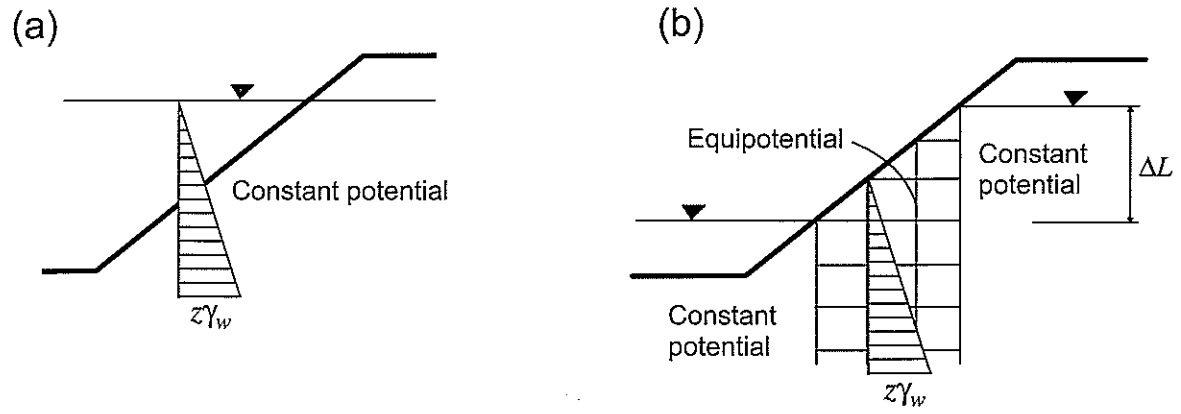

leads to an overestimation of the hydraulic gradients, and it is acceptable for practical calculations (the same assumption was used by Morgenstern 1963).

The strength of the soil is described here by the Mohr–Coulomb yield condition, with ϕ and c being the internal friction angle and cohesion, respectively:

$$[10] \quad f = (\sigma'_x + \sigma'_y)\sin\phi - \sqrt{(\sigma'_x - \sigma'_y)^2 + 4\tau_{xy}^2} + 2c\cos\phi = 0$$

where the prime denotes effective stresses, and τ_{xy} is the shear stress. The most adverse failure mechanism of a uniform slope is that of a rigid rotation with the failure surface described by a logarithmic spiral (Chen 1975), as presented in Fig. 3. Both the toe failures and under-the-toe mechanisms of collapse (characteristic of shallow slopes) are considered here. In the latter, the soil below the toe is assumed to have the same characteristics as that in the slope.

The upper bound to the dimensionless critical height ($\gamma H/c$) of the slope can be derived from the work rate balance equation, or the lower bound to its reciprocal can be found, called here the stability factor ($c/\gamma H$):

$$[11] \quad \frac{c}{\gamma H} = \frac{r_0}{H}\frac{2\tan\phi\left(f_1 - f_2 - f_3 - f_4 + \frac{\gamma_w}{\gamma}f_5\right)}{\exp[2(\theta_h - \theta_0)\tan\phi] - 1}$$

where angles θ_0 and θ_h determine the location of the logarithmic spiral failure surface (Fig. 3); and γ and γ_w are the unit weights of the soil and water, respectively. Coefficients f are dependent on the slope geometry, specific location of the failure surface, and ϕ. The expressions for coefficients f_1–f_4 can be found in Chen (1975) or Michalowski (1995). The influence of both the pore-water pressure and the rapid drawdown is enclosed in coefficient f_5, which follows from the rate of work in eq. [8] applied to the analyzed mechanism. This coefficient does not have a convenient closed form, and it is calculated numerically in this analysis (see Appendix A). The solution to the problem is found through an optimization procedure where the maximum value of $c/\gamma H$ is sought with the geometry of the slip surface being variable. If an earth dam is considered, an assumption is made that the failure surface is enclosed entirely within the cover material (it does not intersect the core of the earth dam).

Fig. 3. Rotational collapse mechanism.

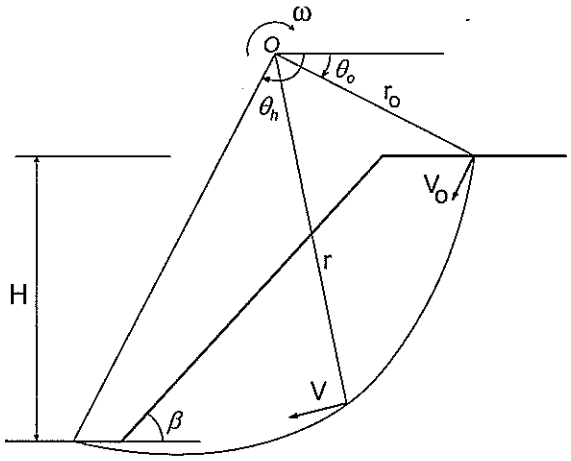

Stability analysis when c = 0

The stability of a slope built with granular material is a special case of the more general case for the cohesive–frictional material considered in the previous section. With a drop in the magnitude of cohesion, the most critical mechanism for a "dry" slope approaches translation along a "shallow" straight-line failure surface, and the analysis in the previous section becomes progressively inaccurate as the center of rotation tends to infinity. Therefore, the translational mechanism for the case $c = 0$ is considered separately here.

The "surficial" sliding is typical of dry sand placed at an angle close to the angle of repose, and it is considered in practice as a maintenance problem rather than failure. For the case of rapid drawdown, however, the problem is not academic, and it is worth pursuing.

A partially submerged slope built out of purely granular soil (no cohesion) is shown in Fig. 4. This is a stage during or immediately after the drawdown, and the assumption of vertical equipotentials within the slope (as in Fig. 2*b*) is used here. The theorem in eq. [9] is used to arrive at the combination of geometry, hydraulic conditions, and soil properties for the slope, which is on the verge of collapse. Because

Fig. 4. Collapse mechanism of a granular slope.

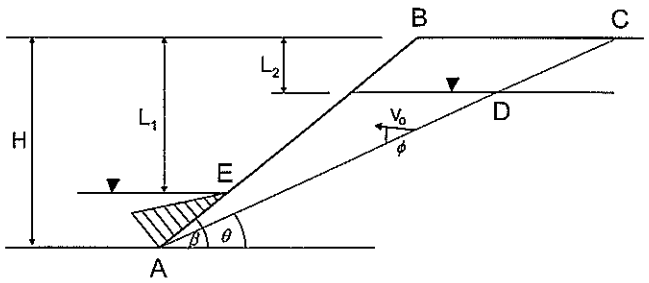

there is no cohesion in the soil, the rate of internal work predicted by the normality rule on the left-hand side of eq. [9] is zero, and the first term on the right-hand-side is zero because traction $T_i = 0$. Hence the theorem can be written here as

$$[12] \quad 0 \geq \dot{W}_\gamma + \dot{W}_u$$

The collapse mechanism consists of one block sliding on surface ADC (Fig. 4), with velocity v_0, and the two terms in eq. [12], $\dot{W}_\gamma$ and $\dot{W}_u$, represent the work rate of the soil weight of block ABC and the effect of water pressure, respectively (work rate of the pore pressure on the soil dilation along the kinematical discontinuity surface AD, and the work rate of the water pressure on the soil surface AE; see Appendix B).

A stable slope (not subjected to seepage forces) requires only that $\phi > \beta$ (where β is the inclination angle of the slope), and therefore the vector of velocity of block ABC, v_0, predicted by the associative flow rule has an upward vertical component. Failure of such a slope cannot be triggered by the soil weight, but it can be caused by additional loads, such as an earthquake load, or the seepage forces due to an increased hydraulic gradient during the rapid drawdown. This effect is captured in the last term in eq. [12]. Upon substitution of the expressions in eqs. [B1]–[B3] (Appendix B) into eq. [12], and after some algebraic and trigonometric transformation, one obtains the following inequality:

$$[13] \quad G = \frac{\gamma_w}{\gamma}\left(1 - \frac{\tan\theta}{\tan\beta}\right) \times \left[\left(1 - \frac{L_2}{H}\right)^2 \frac{\sin\phi}{\cos(\phi - \theta)} - \left(1 - \frac{L_1}{H}\right)^2 \sin\theta\right] + \frac{\sin(\beta - \theta)}{\sin\beta} \tan(\theta - \phi) \leq 0$$

where G is a function of the slope geometry, soil properties, and the collapse mechanism; H is the slope height; and L_1 and L_2 are the levels of water in the reservoir and in the slope measured from the crown level (Fig. 4). The inequality in eq. [13] has been derived using the kinematic theorem of limit analysis, however; therefore, to derive a realistic combination of the parameters for a slope at the brink of failure, one needs to consider the most adverse geometry of the mechanism, when θ approaches β. This indicates a surficial collapse, characteristic of dry granular slopes. Since the condition $\theta = \beta$ substituted directly into inequality [13] produces a trivial solution, we rewrite eq. [13] as

$$[14] \quad G = A + B = 0$$

or

$$[15] \quad B/A = -1$$

and we seek the limit of B/A when $\theta \to \beta$. Using de l'Hôpital's rule, one arrives at the following limit:

$$[16] \quad \lim_{\theta \to \beta} \frac{B}{A} = \frac{\gamma}{\gamma_w} \times \frac{\cos\beta \sin(\beta - \phi)}{(1 - L_2/H)^2 \sin\phi - (1 - L_1/H)^2 \sin\beta \cos(\phi - \beta)}$$

Now, equating the result in eq. [16] to –1 (see eq. [15]), we obtain

$$[17] \quad \tan\phi = \frac{\left[1 - \frac{\gamma_w}{\gamma}\left(1 - \frac{L_1}{H}\right)^2\right] \sin\beta\cos\beta}{\frac{\gamma_w}{\gamma}\left(1 - \frac{L_1}{H}\right)^2 \sin^2\beta - \frac{\gamma_w}{\gamma}\left(1 - \frac{L_2}{H}\right)^2 + \cos^2\beta}$$

or, for a slope of given ϕ and β, the safety factor can be calculated as

$$[18] \quad F = \tan\phi \frac{\frac{\gamma_w}{\gamma}\left(1 - \frac{L_1}{H}\right)^2 \sin^2\beta - \frac{\gamma_w}{\gamma}\left(1 - \frac{L_2}{H}\right)^2 + \cos^2\beta}{\left[1 - \frac{\gamma_w}{\gamma}\left(1 - \frac{L_1}{H}\right)^2\right] \sin\beta\cos\beta}$$

Equation [17] determines a combination of soil and geometrical parameters of the slope, associated with reaching surficial instability, for given water levels L_1 and L_2.

We emphasize that the "surficial" mechanism associated with the solution in eq. [18] may not be the most adverse mechanism for submerged slopes and different drawdown regimes. Therefore, the results from eq. [18] are compared later with those from the analysis presented in the previous section (with $c \to 0$).

Stability charts

A parameter that is most often used to characterize slopes in stability analyses is a stability factor defined as a critical value of $c/\gamma H$. This factor also has been used to define slopes in rapid drawdown calculations (Morgenstern 1963; Lane and Griffiths 2000). The critical value of $c/\gamma H$ was calculated here with a modified computer code used earlier (Michalowski 1995). For a given slope geometry, soil properties, and hydraulic conditions, the best lower bound to $c/\gamma H$ in eq. [11] was found using an optimization procedure (location of the failure surface being variable). This best lower bound to $c/\gamma H$ is called the stability factor, and we denote this factor as N. The safety factor is defined here as

Fig. 5. Four different drawdown regimes for charts shown in Figs. 6–9.

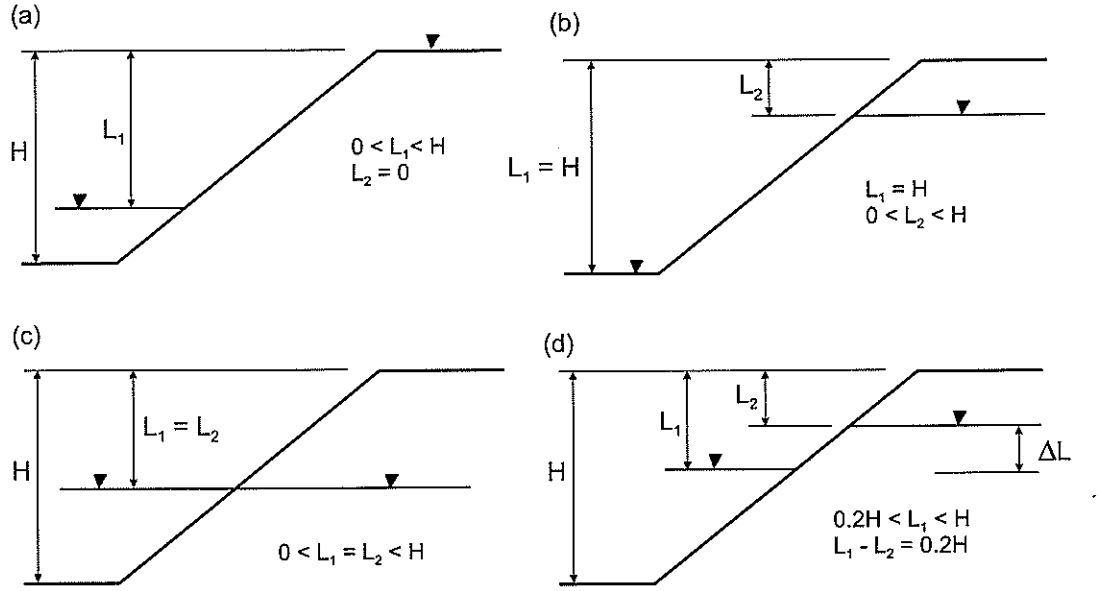

$$[19] \quad F = \frac{c}{c_d} = \frac{\tan\phi}{\tan\phi_d}$$

where c_d and ϕ_d are the soil strength parameters necessary only to maintain the structure in limit equilibrium. The slope with a critical combination of c, γ, and H (i.e., such that $c/\gamma H = N$) has the safety factor $F = 1$.

Typically, if the stability factor $N = c/\gamma H$ is known for a slope of given inclination β and given internal friction angle ϕ, an iterative procedure is required to find the safety factor for a slope of arbitrary combination c, γ, and H, but given β and ϕ. An iterative procedure can be avoided, however, if $F/(\tan\phi)$ is plotted as a function of $c_d/(\gamma H \tan\phi_d)$. This is because parameter $c_d/(\gamma H \tan\phi_d)$ is independent of safety factor F:

$$[20] \quad \frac{c_d}{\gamma H \tan\phi_d} = \frac{c/F}{\gamma H(\tan\phi/F)} = \frac{c}{\gamma H \tan\phi}$$

Hence, estimation of the safety factor from charts presented as functions of $c_d/(\gamma H \tan\phi_d)$ (or $c/(\gamma H \tan\phi)$) will not require any iterative procedures. This method of presenting the results was proposed earlier by Bell (1966) and was used recently to present charts based on limit analysis (Michalowski 2002).

Four sets of stability charts are shown in this paper for different conditions of rapid and slow drawdown processes characterized by a varied relative location of water levels indicated in Fig. 5. The specific regimes indicated in Figs. 5*a*–5*d* relate to the charts in Figs. 6–9, respectively. The limit analysis leading to the solution in eq. [11] becomes singular when $c = 0$, and therefore the solution in eq. [18] is used in some cases. It was found, however, that for granular slopes and some drawdown regimes the surficial failure mechanism used to develop this solution for $c = 0$ is not the most adverse collapse mode. In these cases the charts are not extended to very small values of $c/(\gamma H \tan\phi)$.

The safety factor for a rapid drain of water from its highest possible level ($L_1 = L_2 = 0$) to complete drawdown ($L_1 = H$) is presented in the charts in Fig. 6. The four separate charts are for four different slope inclinations (vertical to horizontal = 1:1, 2:3, 1:2, and 1:3). The results for the steeper slopes (1:1) may be useful in estimating the safety of slopes built for flood protection or river banks, whereas the more gentle slopes are more typical of earth dams.

Relatively large values of the parameter $c/(\gamma H \tan\phi)$ (larger than 0.5) are characteristic of low slopes built using soil with a small internal friction angle, e.g., $c/(\gamma H \tan\phi) = 0.71$ when $c = 25$ kPa, $\gamma = 20$ kN/m^3, $H = 10$ m, and $\phi = 10°$. Small values of $c/(\gamma H \tan\phi)$ describe higher slopes built using soils with lower cohesion but larger internal friction angle, e.g., $c/(\gamma H \tan\phi) = 0.03$ when $c = 10$ kPa, $\gamma = 18$ kN/m^3, $H = 50$ m, and $\phi = 25°$. Therefore, charts are presented for values of $c/(\gamma H \tan\phi)$ ranging from 0 to 0.8; in addition, separate charts for the range 0–0.1 are also shown.

The curves in each chart represent the safety factor F divided by $\tan\phi$ (i.e., $F/(\tan\phi)$) as a function of the parameter $c/(\gamma H \tan\phi)$, each curve for one specific depth L_1/H of the water table (while $L_2 = 0$). These are all numerical results, and different symbols are used to identify each curve. The results are from calculations using eq. [11] for an optimized failure mechanism, except when $c/(\gamma H \tan\phi) = 0$, where eq. [17] was used. As expected, the safety factor decreases with an increase in the depth of water table L_1.

The second set of charts (Fig. 7) is for evaluation of the increase in the safety factor after the reservoir has been rapidly drained, i.e., increasing L_2 while $L_1 = H$. Not surprisingly, the safety factor is now increasing with an increase in depth L_2. It is interesting to note that the shallow translational failure is not the most adverse mechanism for this case when c approaches zero, and the calculation points close to $c/(\gamma H \tan\phi) = 0$ (between 0 and 0.01) were all obtained from logarithmic-spiral mechanisms.

The third set of charts (Fig. 8) is for a very slow drawdown, where the difference in water level in the reservoir and the slope can be neglected ($L_1 \approx L_2$). As illustrated later in the paper, the process starts with the maximum safety factor, and the minimum is reached somewhere before the res-

Fig. 6. Rapid-drawdown charts ($L_2 = 0$).

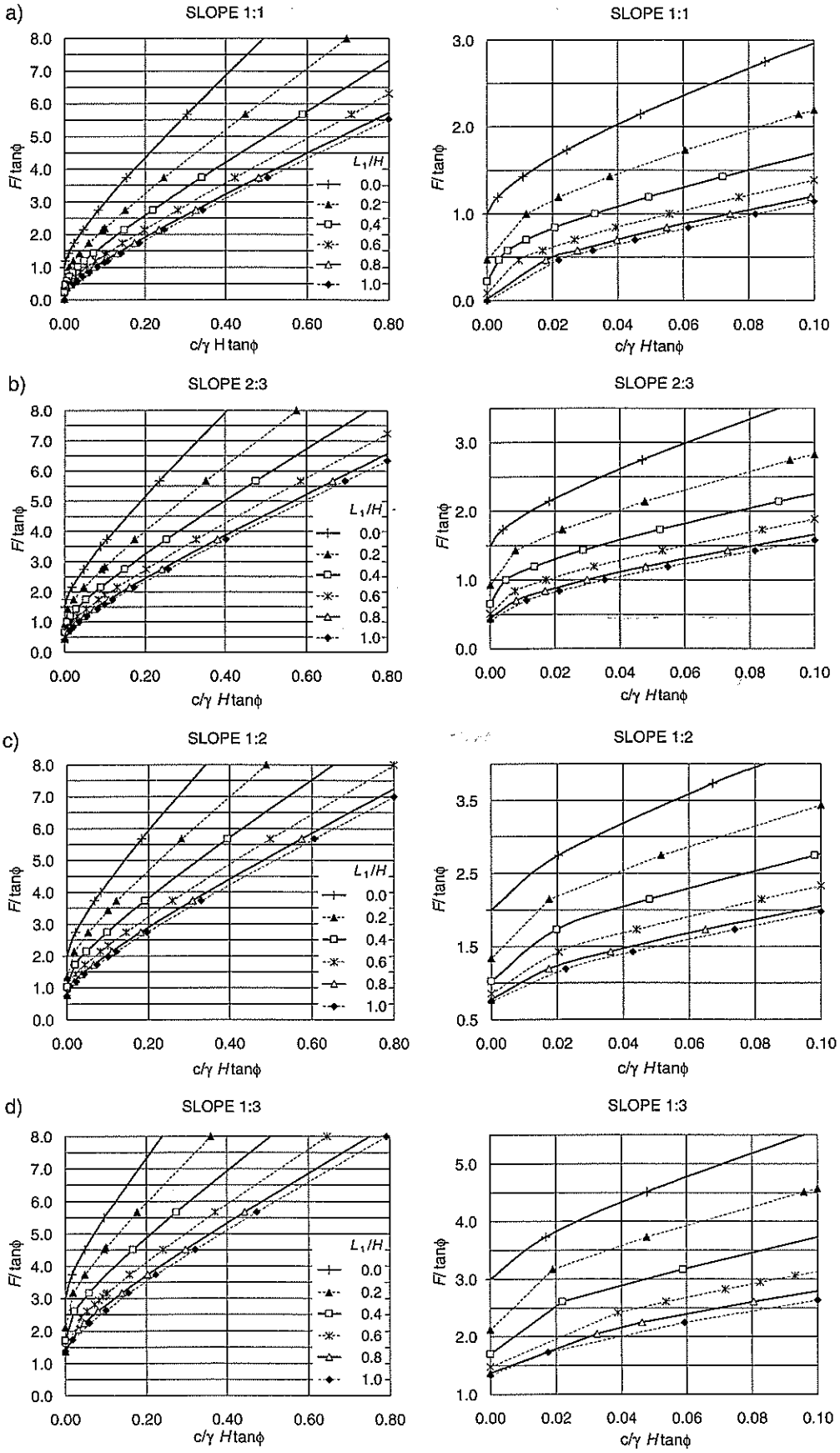

Fig. 7. Effect of the drop of the phreatic surface depth L_2 for a fully drained reservoir ($L_1 = H$).

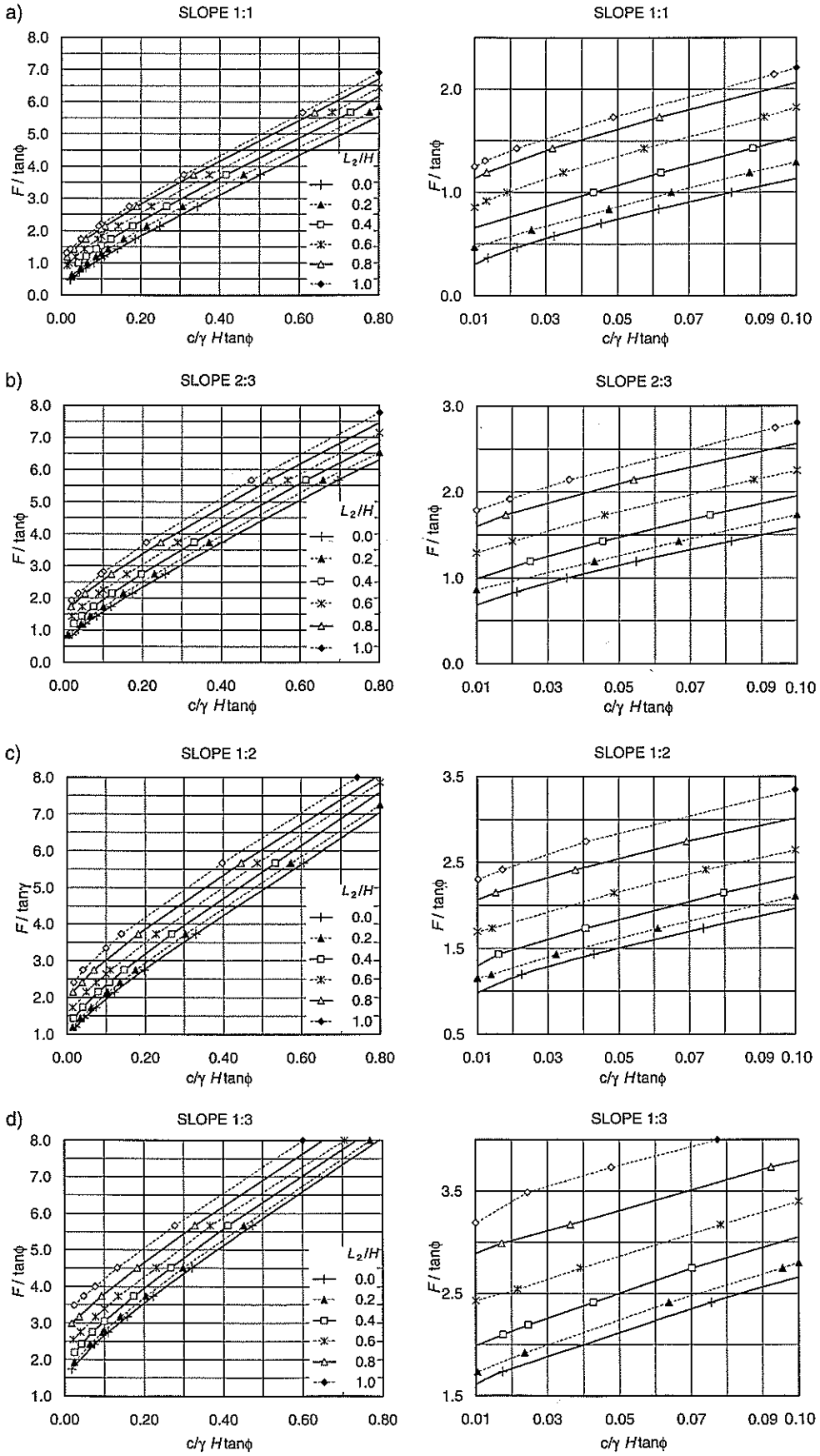

Fig. 8. Safety factor for a very slow drawdown ($L_1 = L_2$).

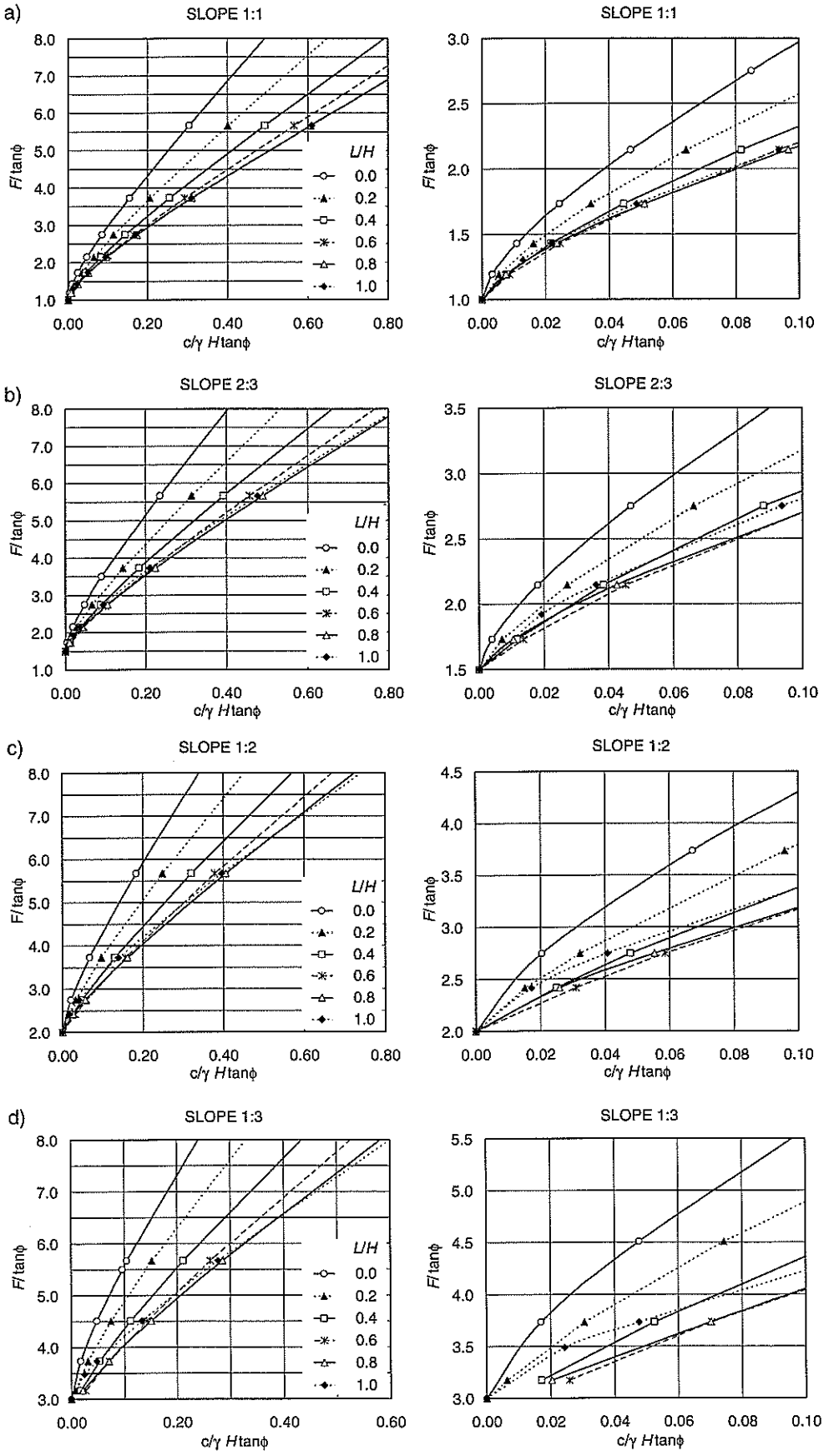

Fig. 9. Safety factor for a drawdown process with a constant drop in water levels ($L_1 - L_2 = 0.2H$).

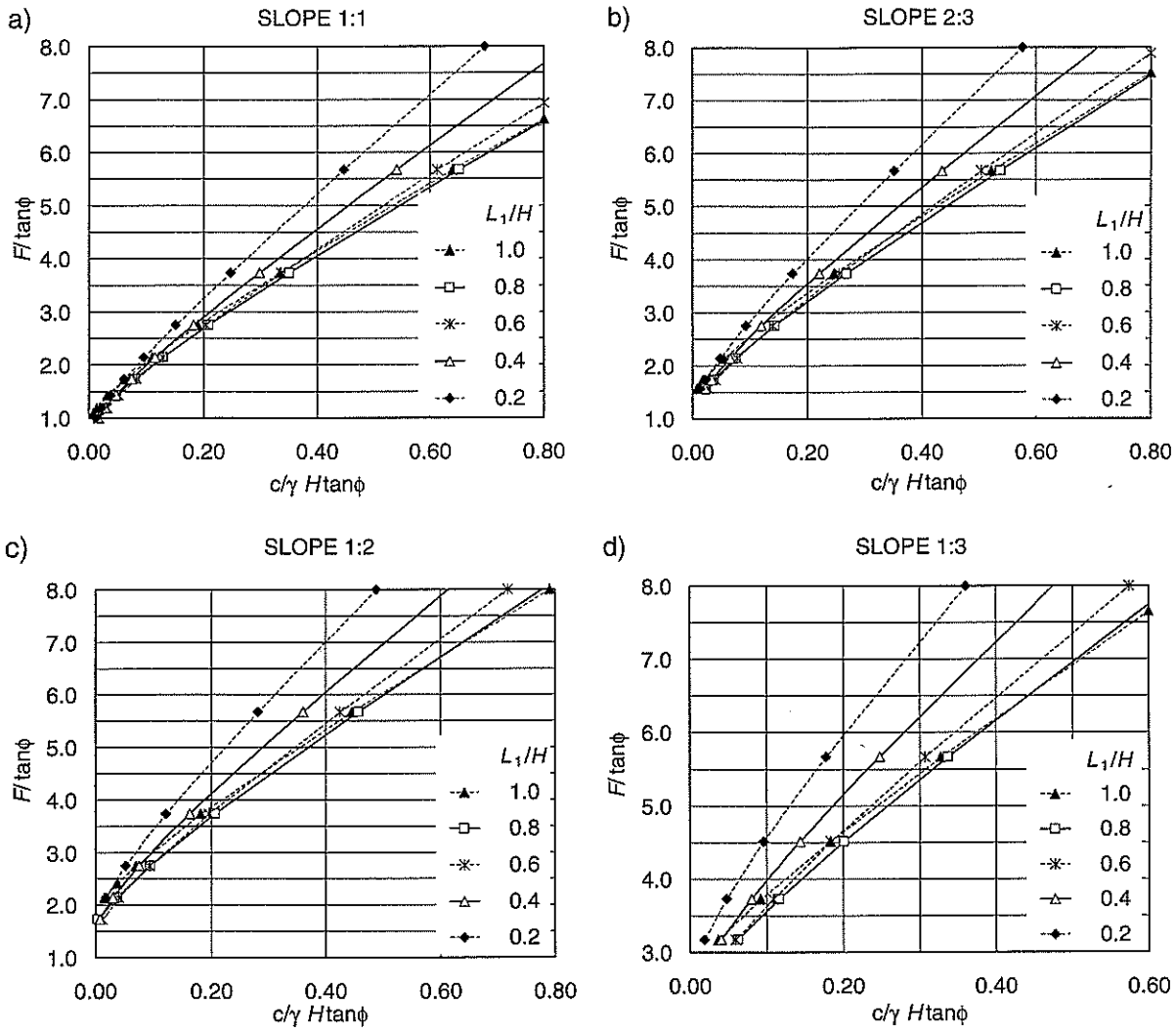

ervoir is completely drained. There seems to be some anomaly in the results for a flat slope (1:3) and small $c/(\gamma H \tan\phi)$. This is caused by the influence of pore-water pressure in the below-the-toe mechanisms that are characteristic of "shallow" slopes. For granular soils ($c = 0$) and gentle slopes, the logarithmic-spiral mechanism yields values of F considerably lower than that from the shallow translational mechanism characteristic of dry granular slopes.

The last set of charts (Fig. 9) is for the draining process, where the drop in water level in the reservoir and in the slope is kept constant ($L_1 - L_2 = 0.2H$). Again, it is shown later in the paper that the safety factor during this drawdown mode has its maximum at the beginning of the process and reaches its minimum somewhere before the reservoir is completely drained. For this drawdown regime (and soil with $c = 0$), the logarithmic-spiral failure surface was a more adverse mechanism than the shallow translational mechanism.

Comparison with other results

The changes in the safety factor associated with different draining regimes are presented in Fig. 10 for a slope with inclination 1:2, $c/\gamma H = 0.05$, and $\phi = 40°$. The rapid drawdown is indicated by the curve marked with open diamonds. Morgenstern's (1963) results for the rapid drawdown are nearly identical to those from the kinematic limit analysis presented here, even though the technique used by Morgenstern was based on the method of slices (Bishop and Morgenstern 1960). Morgenstern's results are not shown in Fig. 10 to avoid cluttering the graph (incidentally, the results are mislabeled in the original paper of Morgenstern 1963). The slow drawdown process is shown by the curve marked with open circles. This is the safest process for emptying the reservoir. A faster process, with a constant difference in water levels ($L_1 - L_2 = 0.2H$, solid triangles) is characterized by slightly lower safety factors, but it is far safer than the rapid drawdown process. If the water is drawn rapidly from the reservoir (open diamonds), the subsequent change in the phreatic surface in the slope leads to an increase in the safety factor, as indicated by the curve marked with solid squares. All of these regimes can be simulated using the charts in Figs. 6–8.

For two drawdown processes, marked in Fig. 10 with open circles and solid triangles, the safety factor reached its minimum at about $L/H \approx 0.65$ and 0.70, respectively. This is

Fig. 10. Variation in safety factor caused by various drawdown processes for slope 1:2, $c/\gamma H = 0.05$, and $\phi = 40°$.

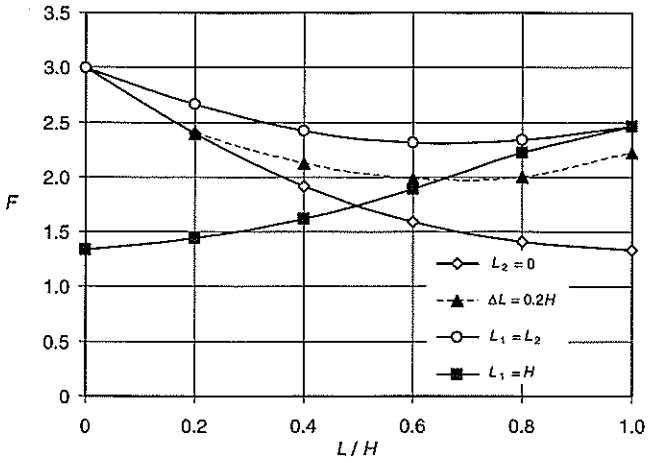

Fig. 11. Comparison of the rapid-drawdown results ($L_2 = 0$, $c/\gamma H = 0.05$) with the finite element calculations.

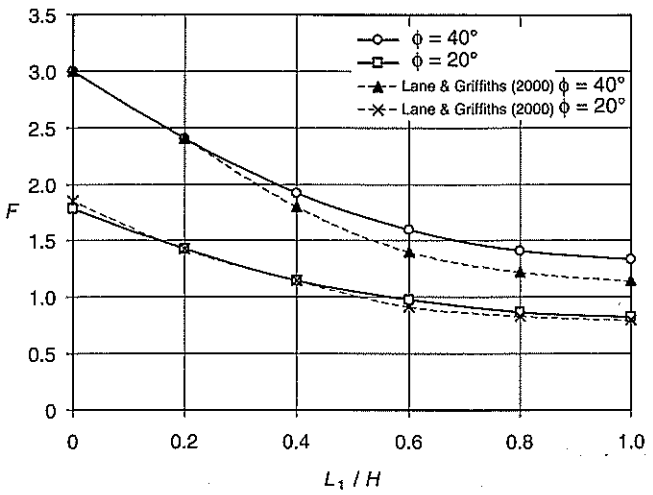

an interesting phenomenon indicating that the extreme states of full submergence and the state after full drawdown may be safe states, whereas the slope becomes most vulnerable to collapse somewhere before the reservoir is fully drained. The appearance of this critical pool level was pointed out by Lane and Griffiths (1997), and they offered an explanation of this phenomenon (Lane and Griffiths 2000) as a result of two competing effects, namely the change in the load of the slope (due to buoyancy) and the change in the frictional resistance of the soil, both caused by the varying level of water.

Comparison of the calculated variation of the safety factor during a rapid drawdown with that from finite element analysis (Lane and Griffiths 2000) is presented in Fig. 11 for a slope with an inclination of 1:2 and $c/\gamma H = 0.05$, and for two values of ϕ, namely 20° and 40°. The results for $\phi = 20°$ coincide very closely, whereas the safety factor for $\phi = 40°$ reaches a maximum difference of about 14% at the end of the process. Although this difference is not unreasonable, we point to the difference in the soil model used in both methods as an explanation for this deviation. The limit analysis is based on the perfect plasticity model with the yielding described by the Mohr–Coulomb function and the deformation governed by the normality rule (associativity). The calculation of Lane and Griffiths (2000), on the other hand, included the soil model with the nonassociative flow rule (incompressible material). Since nonassociativity leads to reduced limit loads on a structure (Rádenkovic 1962), one would expect the nonassociative model to provide lower safety factors.

Final remarks

The kinematic approach of limit analysis was applied to the problem of stability of submerged (or partially submerged) slopes and subjected to a process of water drawdown. The results are presented as generic charts and allow one to calculate the variation of the safety factor for a slope subjected to a rapid or slow drawdown. The charts produced are convenient to use, and they allow one to estimate the safety factors during drawdown from full or partial submergence.

Although the safety factor can be estimated using the charts for the specific water levels in the reservoir (or over a floodplain) and in the slope, the true rate of the process of draining water from soil is dependent on the rate of reservoir draining and the hydraulic conductivity of the soil. The depth of the water table in the reservoir and in the soil must be known before the safety factor can be determined from the charts. These levels can be obtained from observation, and the charts can be used to actively control the process of draining.

During a rapid drawdown the safety factor reaches its minimum when the water level in the reservoir reaches its minimum (fully drained stage). When the drawdown process occurs at a slower rate, however, the slope becomes most vulnerable to collapse some time before reaching the fully drained stage. In the example presented in the paper, the safety factor reached its minimum when the water level in the basin dropped by about 70% of its original height (65% for a very slow process). This critical pool level can be determined from the charts presented in the paper.

It was interesting to notice that the shallow sliding (translational) mechanism associated with the minimum safety factor for dry granular slopes is not the most adverse collapse pattern for granular slopes subjected to all drawdown regimes. A separate study addressing collapse mechanisms of slopes built of granular soils will be undertaken in the future.

Acknowledgements

The work presented in this paper was carried out while Prof. Michalowski was supported by the US National Science Foundation grant CMS-0096167 and the US Army Research Office grant DAAD19-03-1-0063, and Mr. Viratjandr was supported by the Royal Thai Government Scholarship. This support is greatly appreciated.

References

Bell, J.M. 1966. Dimensionless parameters for homogeneous earth slopes. Journal of the Soil Mechanics and Foundations Division, ASCE, **92**: 51–65.

Bishop, A.W., and Morgenstern, N.R. 1960. Stability coefficients for earth slopes. Géotechnique, **10**: 129–150.

Chen, W.F. 1975. Limit analysis and soil plasticity. Elsevier, Amsterdam, The Netherlands.

Lane, P.A., and Griffiths, D.V. 1997. Finite element slope stability analysis. *In* Proceedings of the 6th International Symposium on Numerical Models in Geomechanics (NUMOG VI), Montréal, Que., 2–4 July 1997. A.A. Balkema, Rotterdam, The Netherlands. pp. 589–593.

Lane, P.A., and Griffiths, D.V. 2000. Assessment of stability of slopes under drawdown conditions. Journal of Geotechnical and Geoenvironmental Engineering, ASCE: **126**(5): 443–450.

Michalowski, R.L. 1995. Slope stability analysis: a kinematical approach. Géotechnique, **45**: 283–293.

Michalowski, R.L. 1999. Stability of uniformly reinforced slopes. Closure. Journal of Geotechnical and Geoenvironmental Engineering, ASCE, **125**(1): 84–86.

Michalowski, R.L. 2002. Stability charts for uniform slopes. Journal of Geotechnical and Geoenvironmental Engineering, ASCE, **128**(4): 351–355.

Morgenstern, N. 1963. Stability charts for earth slopes during rapid drawdown. Géotechnique, **13**: 121–131.

Rádenkovic, D. 1962. Théorie des charges limites extension a la mécanique des sols. *In* Séminaire de Plasticité, 1961. *Edited by* J. Mandel. No. NT 116, Publication Scientifique et Technique de Ministère de l'Air, École Polytechnique, Paris. pp. 129–141.

Terzaghi, K., and Peck, R.B. 1948. Soil mechanics in engineering practice. John Wiley & Sons, Inc., New York.

Wright, S.G., and Duncan, J.M. 1987. An examination of slope stability computations procedures for sudden drawdown. Report GL-87-25, US Army Corps of Engineers, Waterways Experiment Station, Vicksburg, Miss.

Wright, S.G., and Duncan, J.M. 2003. Engineering design — slope stability. Engineer Manual EM 1110-2-1902, US Army Corps of Engineers, Washington, D.C.

Appendix A

The details of calculating coefficients f_1–f_4 in eq. [11] have been explained in Chen (1975), whereas coefficient f_5 is calculated in a manner similar to that in Michalowski (1995) but with some differences because the pore pressure coefficient r_u is not used here and the slope is now fully or partially submerged. No closed-form solution was obtained for coefficient f_5, and the method used to calculate this coefficient is described in the following. The intermediate derivation steps are omitted, however. Coefficient f_5 originates from the last two terms of eq. [9]. The geometrical quantities used in calculating f_5 are presented in Fig. A1. In general terms, the work of the pore-water pressure and water pressure on the boundary during rigid rotation with angular velocity ω about point O (Fig. A1) can be written as

Fig. A1. Notation for analysis of a partially submerged slope.

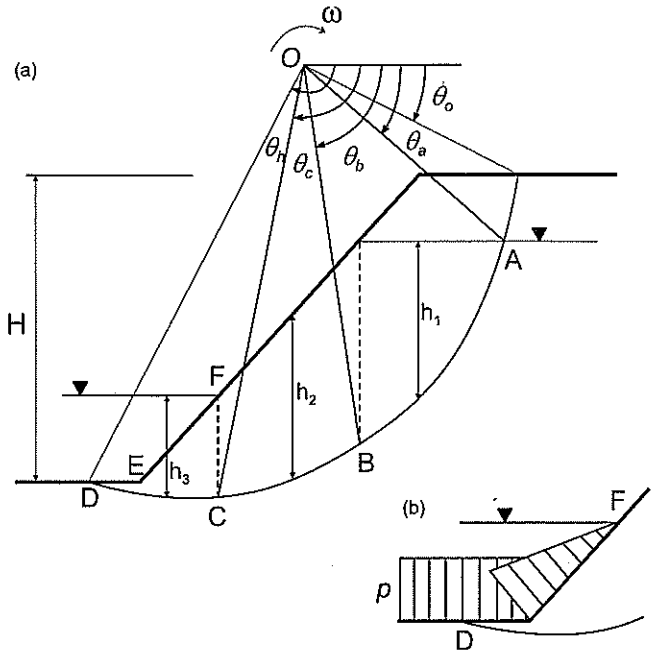

[A1] $$\dot{W}_u = \gamma_w r_0^2 \omega \tan\phi \left\{ \int_{\theta_a}^{\theta_b} h_1 \exp[2(\theta-\theta_0)\tan\phi]\,d\theta + \int_{\theta_b}^{\theta_c} h_2 \exp[2(\theta-\theta_0)\tan\phi]\,d\theta + \int_{\theta_c}^{\theta_b} h_3 \exp[2(\theta-\theta_0)\tan\phi]\,d\theta \right\} - \int_{BC} pn_i v_i\,dS - \int_{CD} pn_i v_i\,dS$$

where p is the water pressure along the boundary DEF, n_i is the outward unit vector perpendicular to the boundary DEF, and v_i is the velocity vector along that boundary. Coefficient f_5 can be reduced to a general form

[A2] $$f_5 = \frac{\dot{W}_u}{\gamma_w r_0^3 \omega}$$

with $\dot{W}_u$ evaluated numerically from eq. [A1].

Appendix B

The rate of work of the soil weight of block ABC (Fig. 4) moving with velocity v_0 during incipient failure is

[B1] $$\dot{W}_\gamma = v_0 \frac{\gamma H^2}{2} \frac{\sin(\beta-\theta)\tan(\theta-\phi)}{\sin\theta\sin\beta}$$

The rate of work of the pore-water pressure on section AD of surface AC was found to be

$$[B2] \quad \dot{W}'_u = v_0 \left[\frac{\gamma_w (H - L_1)^2}{2} \frac{\sin\phi}{\tan\beta \cos\theta \cos(\phi - \theta)} + \frac{\gamma_w (H - L_2)^2}{2} \left(1 - \frac{\tan\theta}{\tan\beta}\right) \frac{\sin\phi}{\sin\theta \cos(\phi - \theta)} \right]$$

and the work rate of the water pressure on boundary AE is

$$[B3] \quad \dot{W}''_u = -v_0 \frac{\gamma_w (H - L_1)^2}{2} \frac{\sin(\phi + \beta - \theta)}{\sin\beta \sin(\phi - \theta)}$$

The sum $\dot{W}'_u + \dot{W}''_u$ is the total water pressure effect $\dot{W}_u$ in eq. [12].